FATIGUE BEHAVIOUR OF HSC AND UHPFRC BEAMS WITH HIGH GRADE STEEL REINFORCEMENT

RANDL Norbert [1], MÉSZÖLY Tamás [2], HARSÁNYI Peter [3]

Abstract

Two series of HSC and UHPFRC beams reinforced with high grade steel bars were tested under high-cycle fatigue loading. In the first series the behaviour of beams made of high strength concrete (HSC) with rectangular cross sections and with a compression strength of 113 MPa was investigated. In the second series beams made of ultra-high strength fibre reinforced concrete (UHPFRC) with I-shaped cross sections and 2 vol% of fibres were tested. The compression strength measured on 100 mm cubes was around 170 MPa. Based on the full material characterization (compression, modulus of elasticity, uniaxial, splitting and flexural tensile tests) the constitutive law for the UHPFRC was derived. In both series S670/800 high grade steel longitudinal reinforcing bars were used. The reinforcement ratio was 2.7% for the HSC and 3.0% for the UHPFRC beam members. The maximum force of the pulsating load applied to the four-point test setup varied between 35% and 70% of the monotonic load bearing capacity. All tests resulted in fatigue failure of the longitudinal reinforcement and maximum cycle numbers between 3×10^4 and 2×10^6 were reached. Comparing the load bearing behaviour of the HSC and UHPFRC beams, the numbers of endured load cycles were noticeably higher for UHPFRC beams. Obviously the fibres in the UHPC played an important role, taking over part of the tensile force and thus reducing the stress amplitude in the longitudinal reinforcement.

Keywords: Fatigue failure, Ultra-High Performance Concrete, HSC, UHPFRC, steel fibre reinforcement, high grade steel

1. Introduction

In comparison with normal strength concrete (NSC), High Strength Concrete (HSC) and Ultra-High Performance Concrete (UHPC) fail in a much more brittle way. In order to obtain a less brittle failure in compression and a more ductile structural behaviour, the addition of steel fibres provide an adequate complement for UHPC, resulting in a new material called Ultra-High Performance Fibre Reinforced Concretes (UHPFRC). Due to the pronounced slenderness of UHPFRC members, fatigue failure plays a more important role than in ordinary RC design when loaded under cyclic conditions.

[1] RANDL Norbert, Carinthia University of Applied Sciences, Villacher Strasse 1, Spittal an der Drau A-9800, Austria, n.randl@cuas.at

[2] MÉSZÖLY Tamás, Carinthia University of Applied Sciences, Villacher Strasse 1, Spittal an der Drau A-9800, Austria, meszoly@cuas.at

[3] HARSÁNYI Peter, Carinthia University of Applied Sciences, Villacher Strasse 1, Spittal an der Drau A-9800, Austria, p.harsanyi@cuas.at

The effect of steel fibre content on the fatigue behaviour in fibre reinforced concrete was already investigated by several other researchers in the last decades. Zhang and Stang [1] found that steel fibre reinforced concrete exhibits superior behaviour and longer fatigue life than plain concrete, and still behaves more ductile. Likewise Barr and Lee [2] described that the addition of fibre reinforcement can increase the fatigue performance of the concrete under flexural fatigue loading due to bridging of cracks. Saleh et al. [3] found that none of the investigated fatigue prediction models provide a good match for measured values. Makita and Brühwiler [4] performed a test series under tensile fatigue loading with Ultra-High Performance Reinforced Concrete combined with steel reinforcing bars and found that hybrid reinforced concrete (HRC, structural member that combines continuous reinforcement and randomly distributed steel fibres) can effectively enhance the fatigue behaviour of the concrete structures.

In the present study the fatigue performance of HSC and fibre-reinforced UHPC beams with high grade steel reinforcing bars was investigated under flexural load. While different cross-sections were used in the two test series (rectangular and I-shaped cross-sections), based on the available measurement data and similar failure characteristics both test series together provide complementary information on structural behaviour of high performance materials in fatigue and the contribution of fibre reinforcement in such cases.

2. Material properties

In the first stage of the research project, high and ultra-high strength concrete mixtures were developed, where cement CEM I 52.5 R for the HSC and CEM I 42.5 R HS for UHPC mixtures were used. Beside the cement, microsilica and silica powder as well as superplasticizer on PCE-basis were used. The water to binder ratio was 0.25 for the HSC and 0.21 for the UHPC mixture. In the case of the fibre reinforced UHPC mixture 2 vol% of fibres were used (15 mm long straight steel fibres with a diameter of 0.2 mm and an aspect ratio equal to 75). The fresh and hardened concrete properties were tested according to the Austrian technical standard ÖNORM EN 12390. The mean value of the 28 days compressive strength measured on cubes with a side length of 100 mm was 113 MPa for the HSC and 188 MPa for the UHPFRC mixture. The mean value of the 28 days splitting tensile strength measured on cylinders with diameter of 100 mm was 6.5 MPa for the HSC and 17.1 MPa for the UHPFRC mixture. Young's modulus was 45.5 GPa in the case of HSC and 49.4 GPa in the case of the UHPFRC mixture. As main tensile reinforcement S670/800 high strength steel with a diameter of 18 mm was provided. The stirrups were prepared from BSt 550 steel with a diameter of 10 mm. Tab.1 contains the nominal (i.e. characteristic) values of the steel properties provided by the manufacturers. The mean strength values are about 10% higher.

Tab.1: Properties of the reinforcements

Properties	BSt 550	S 670/800
Ultimate tensile strength f_{tk} [MPa]	620	800
Characteristic yield strength f_{yk} [MPa]	550	670
Young's modulus E_s [GPa]	200	205
Density γ [kg/m^3]	7850	7850

3. Structural tests

3.1 Test specimens

Two series of one-span concrete beams were produced for the fatigue tests. The first series contained beams with rectangular cross sections of 150 mm by 250 mm. Four 18 mm bars steel grade S670/800 have been provided as longitudinal reinforcement. The stirrups were prepared from BSt 550 steel with a diameter of 10 mm (see Fig. 1).

The second series contained beams with I-shaped cross-section with an outer dimension of 200 mm by 350 mm. Five 18 mm bars S670/800 have been provided as longitudinal reinforcement. The stirrups consisted of 10 mm bars steel grade BSt 550 (see Fig. 2).

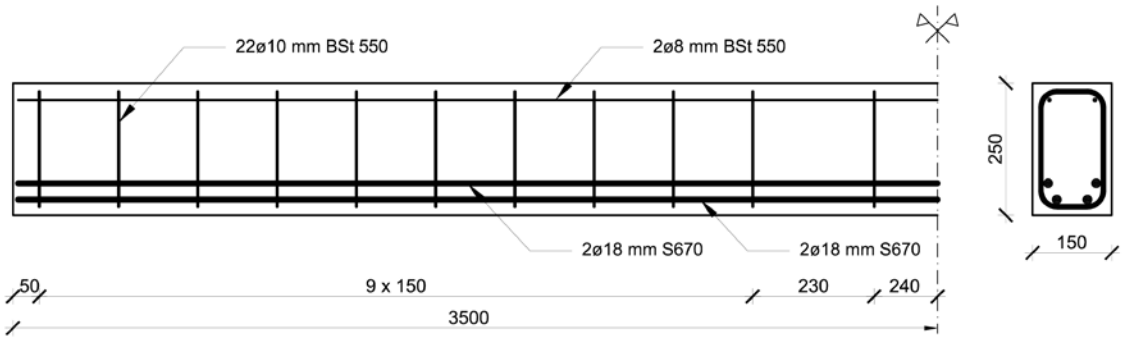

Fig. 1: Reinforcement layout of the rectangular HSC beams

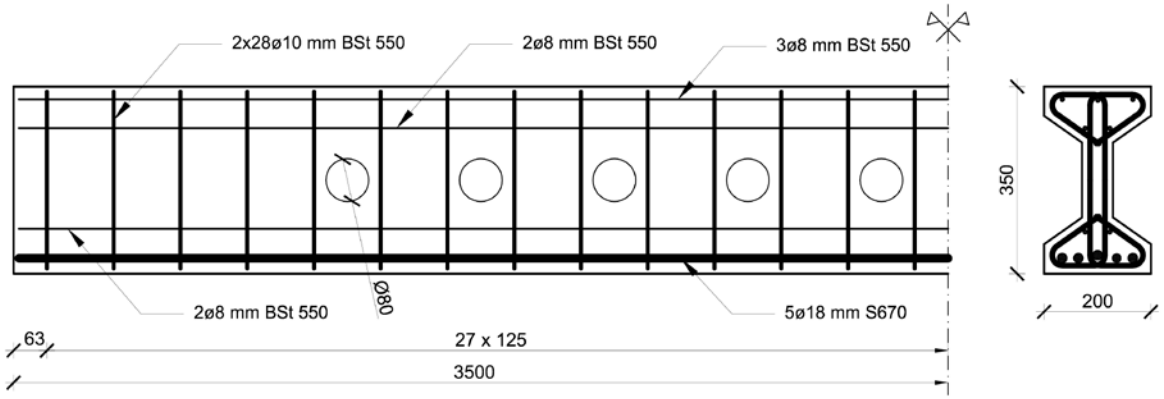

Fig. 2: Reinforcement layout of the UHPFRC beams with I-shaped cross section

3.2 Test setup and testing programme

All beams were tested in a four point bending setup with an identical span of three meters and a distance from support to load introduction of one meter (see Fig. 3). The deformation of the beam was measured by three displacement transducers under the load introduction points and at the middle of the beam. In the middle of each HSC and UHPFRC beam, three strain gauges (DMS) were glued on the top of the compression zone, and a pair of strain gauges was installed on the middle reinforcing steel bar in the tensile zone. A total number of 9 strain gauges in three groups were additionally placed on the web surface of each UHPFRC beam in the shear region (Fig. 4) in order to detect the direction and magnitude of the main principal strains.

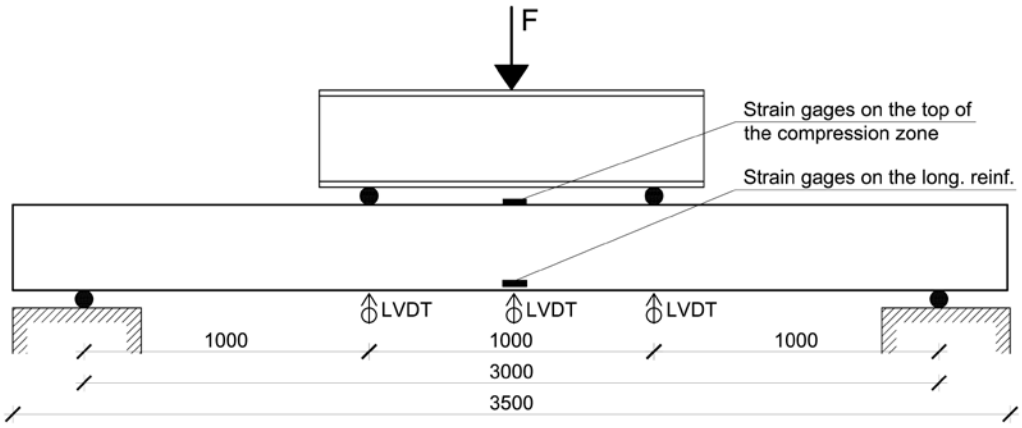

Fig. 3: Four point bending setup

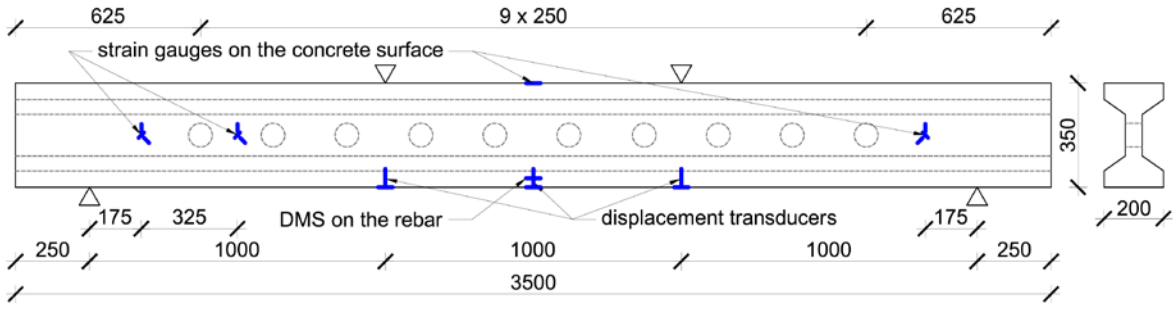

Fig. 4: UHPFRC beam with the measurement units

As a reference one HSC and three UHPFRC beams were tested displacement controlled under monotonic loading until failure to identify the maximum load bearing capacity of each beam type. The maximum reached load was 262 kN for the HSC and 705 kN in average for the UHPFRC beams (scatter of the results was quite low with the coefficient of variation of 1.2%).

The fatigue tests were performed at frequencies around 3 Hz, however varying from 1 to 5 Hz depending on the deflection at each stage. For the HSC beams, during the first load cycle the test was temporarily stopped at the upper load level to record all cracks on the basis of visual inspection and measure the crack widths by means of a crack magnifier.

The UHPFRC beams were subjected to a preloading phase of 3 full load cycles before the high-cyclic fatigue loading started. During the initial cycle, at predefined load steps (75-150-245-350-455 kN depending on the upper limit (F_{ult}) of the following cyclic loading) the crack pattern, crack propagation and the crack width were measured. Afterwards the beams were subjected to three complete load cycles and the crack propagation and crack width were measured again. In the cyclic testing phase the UHPFRC beams were tested with 2-4 Hz and with constant applied load cycles. To determine the progress of crack development, the tests were stopped after every 10^4, 5×10^4 or 10^5 cycles and all crack changes were recorded at the upper limit of the cyclic loading. Maximum and minimum load values and amplitudes of the applied force in percentage of the ultimate load are listed in Tab.2. The level of the minimum loads was below the cracking load whereas the maximum loads were significantly above. The related steel stress values in the longitudinal reinforcing bars remained below the yield strength.

Tab.2: Testing program and the reached cycle numbers

specimen	F_{ult} [kN]	Cyclic loading [kN]	$\Delta F/F_{ult}$ [%]	No. of load cycles
HSC_ref	262			
HSC_1		13-183	65	29,497
HSC_2		20-170	57	56,647
HSC_3		20-150	50	71,187
HSC_4		20-118	38	182,297
HSC_5		20-92	27	838,109
UHPFRC_refs	705			
UHPFRC_1		35-455	60	59,437
UHPFRC_2		35-350	45	193,967
UHPFRC_3		35-280	35	313,302
UHPFRC_4		35-245	30	1,896,866

3.3 Test results and failure mode

All beams were tested until fatigue failure. The reached cycle numbers at failure were between around 3×10^4 and 2×10^6, as shown in Tab.2. The final failure mode was in all cases fatigue rupture of the longitudinal reinforcing steel bars.

Based on the measured data, during cyclic testing the observed load-deflection response can be subdivided into three different phases. During the first several thousand cycles, the deformation of the beam was slightly increasing. In parallel, the strain in the longitudinal reinforcement increased at both lower and upper load levels, but more pronounced at the lower load levels. Therefore the steel stress amplitude slightly decreased despite of the constant load amplitude. On the other hand, the strain in the compression zone of the concrete somewhat increased at upper load level and slightly decreased at the lower load. This first period was followed by a long stable phase, where none of the measured values (deflections and strain values, crack widths, crack heights) changed significantly. The last phase was usually announced by a steady increase of the deformation of the beam and the strains in the reinforcing bars. After several thousand cycles rupture of one of the longitudinal steel bars was observed. Then, after a short stabilization of the structural response, another reinforcing bar failed, shortly followed by the third one. This was accompanied by a pronounced opening of the main bending crack which propagated rapidly into the compression zone of the beam.

One UHPFRC beam, i.e. No. 3, behaved somewhat different: Despite of the symmetric test setup and load introduction, the recorded deformation and strain values as well as the forming crack pattern were different on the two sides of the beam, indicating an unintentional torque loading. Because of this effect the strain of the longitudinal reinforcement in one side was somewhat higher than expected and resulted in an earlier

fatigue failure (see also the next chapter). Having investigated the failure surface, this phenomenon could be deduced to the extremely inhomogeneous fibre distribution with all the fibres concentrated on one side of the beam (in the relevant cross-section).

4. Discussion

As the failure mode under fatigue loading was in all cases rupture of the longitudinal reinforcing bars, a comparison of the results from the HSC and UHPFRC beams is reasonable as always the same type of steel bars with the same diameter was used. The stress amplitudes of the longitudinal reinforcing bars in the lowest position (where the steel stress was highest and therefore first fatigue failure happened) were calculated for the HSC beams according to Eurocode 2 [5] on the basis of actual geometry and mean material data. The results of this calculation are shown in Tab.3 and also depicted in Fig. 5.

Tab.3: Calculated stress amplitudes in the reinforcing bars for HSC beams

specimen	$\Delta\sigma_{calc}$ [MPa]
HSC_1	555.6
HSC_2	490.2
HSC_3	424.9
HSC_4	322.4
HSC_5	235.3

Tab. 4 shows for the UHPFRC beams at different load levels in the second column the recorded steel stress values $\sigma_{m.mon}$ (back-calculated from the measured strain values) in the longitudinal steel bars during the very first monotonic ramp. The force related to the cracking moment was around 60 kN, therefore at the first loading, at 35 kN the cross-section was still uncracked and the related measured stress value (17 MPa) is quite small compared to the other values.

Tab.4: Stress values in the longitudinal reinforcement and in the fibres under monotonic loading for UHPFRC beams

F_{appl} [kN]	$\sigma_{m.mon}$ [MPa]	$\sigma_{cal.wof}$ [MPa]	$\sigma_{cal.wf}$ [MPa]	σ_{cf} [MPa]
35	17	13.5	13.5	0
245	284	324.5	291.7	2.5
280	328	370.9	333.4	2.9
350	417	463.6	416.7	3.6
455	551	602.7	541.7	4.7

The other steel stress values given in Tab. 4 have been back-calculated from the applied force based on the assumption of a linear stress distribution of the UHPFRC compression zone. Thereby the $\sigma_{cal.wof}$ values represent the calculated steel stress for a fictitious UHPC beam with the same setup and amount of longitudinal reinforcement, but without fibres. As expected, the steel stresses in the reinforcing bars would then be significantly higher (9-13%) than the measured ones from the UHPFRC beams. The derived difference also fits to the conclusion from [7] that the contribution of the fibres in case of this material, type of structure and test setup is around 11% at ultimate limit state.

For taking into account the effect of the fibres a simplified calculation model according to Leutbecher and Fehling [6] was used (see Fig. 5). This calculation uses an average residual stress value (σ_{cf}) in the cracked concrete part of the cross-section, which comes from the fibres bridging the cracks. This stress value can be determined as a function of the crack opening by uniaxial tensile, splitting tensile or flexural tests using so-called back-analysis (or inverse analysis). These test results and the derived constitutive law for the particular material are described in detail in [7]. The results based on this calculation model at the given load levels are shown in Tab.4, where $\sigma_{cal.wf}$ is the stress in the lowest reinforcing steel bars considering the fibre effect and σ_{cf} is the average residual tensile stress in the cracked part of the cross-section. According to this calculation the effective values of the average residual tensile stresses due to the fibres were between 0 MPa (uncracked stage) and 4.7 MPa at the given load levels (higher values at higher load levels, see Tab.4).

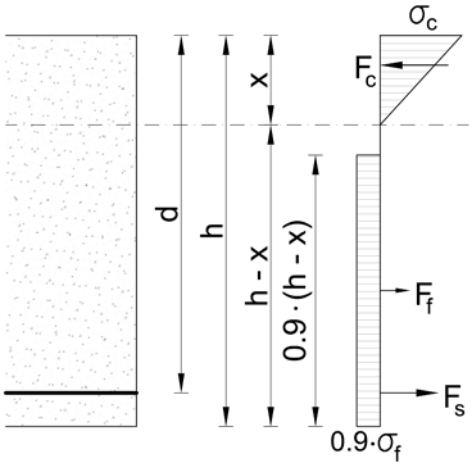

Fig. 5: Simplified calculation model according to Leutbecher and Fehling [6]

As described before, in the first phase of the cyclic loading the stresses in the reinforcing bars were increasing and then stabilized until the last phase of the tests. The values $\sigma_{m.3cyc}$ in Tab. 5 show the steel stresses back-calculated from the measured strains after the first three load cycles, and $\sigma_{m.cyc}$ in Tab. 5 represents the steel stress back-calculated from representative measured strain values during the stabilized phase of the test. The comparison of these values shows 1.4 to 12% increase of the steel stress during cycling; more pronounced at the lower load level and rather small at the upper load levels.

In the first phase of the cyclic loading several effects related to material properties and structural characteristics affected load-deflection response. One of the phenomena is the partial pull-out of the fibres and related degradation of the tensile stress coming from the fibres bridging the cracks.

Using the simplified calculation model as described above, together with the measured strain values of the longitudinal reinforcing bars and the strain values in the compression zone of the concrete, the contribution of the fibres under cyclic loading can be identified. Tab.5 gives the calculated tensile stress in the reinforcing bars ($\sigma_{cal.wf.cyc}$) and the residual tensile stress in the cracked part of the cross-section ($\sigma_{cf.cyc}$). According to this approach the contribution of the fibres under long-term cyclic loading was around 60% lower than under monotonic loading. It has to be mentioned, that there are in addition several other effects which are not taken into account in this simplified approach and need further investigation.

Tab.5: Stress values in the longitudinal reinforcement and in the fibres under cyclic loading

F_{appl} [kN]	$\sigma_{m.3cyc}$ [MPa]	$\sigma_{m.cyc}$ [MPa]	$\sigma_{cal.wf.cyc}$ [MPa]	$\sigma_{cf.cyc}$ [MPa]
35	109	123	46.4	0
245	288	328	311.7	1.0
280	344	365	356.2	1.1
350	427	433	445.2	1.4
455	555	586	578.8	1.8

Tab.6 shows the amplitudes of the tensile stresses in the longitudinal reinforcing bars under cyclic loading for the four tested UHPFRC beams. The values $\Delta\sigma_{meas}$ represent the calculated stress amplitudes based on the measured strain values, whereas $\Delta\sigma_{calc.wof}$ shows the calculated stress amplitudes for a fictitious UHPC beam with the same setup but without fibres. On the other hand, the values $\Delta\sigma_{calc.wf}$ show the calculated stress amplitudes based on the calculation described before and using the $\sigma_{cal.wf.cyc}$ values from Tab.5, taking into account the effect of the fibres.

Tab.6: Stress amplitudes in the longitudinal reinforcement under cyclic loading

specimen	$\Delta\sigma_{meas}$ [MPa]	$\Delta\sigma_{calc.wof}$ [MPa]	$\Delta\sigma_{calc.wf}$ [MPa]
UHPFRC_1	463	556.3	532.4
UHPFRC_2	310	417.2	398.8
UHPFRC_3	242	324.5	309.8
UHPFRC_4	205	278.1	265.3

The endured stress amplitudes are compared to the current approach for fatigue design as per fib Model Code 2010 [8]. For the main longitudinal reinforcement with diameter 18 mm and steel quality S670/800, the characteristic and mean S-N curves derived on the basis [8] are shown in Fig. 6. In addition the test results, represented by the recorded and

calculated stress amplitudes (calculation process described earlier) are introduced in Fig. 6 versus the endured maximum number of cycles (see Tab.2).

The recorded steel stresses (rhombus-shaped dots for the HSC and circle-shaped dots for the UHPFRC beams in Fig. 6) are quite close to the calculated mean S-N curve for the S670/800 steel: at lower stress amplitude they fit very well and at higher amplitudes the measured values are slightly above. The fatigue results from UHPFRC beams, using the calculated stress amplitudes in Tab.6 and the maximum number of cycles, are significantly above the S-N curve derived from [8] (square-shaped dots depict the results without the fibre effect and triangular-shaped dots show the results with fibre effect). Again, the steel stresses based on the measured values and the reached number of cycles fit well to the fatigue model given in the fib Model Code 2010.

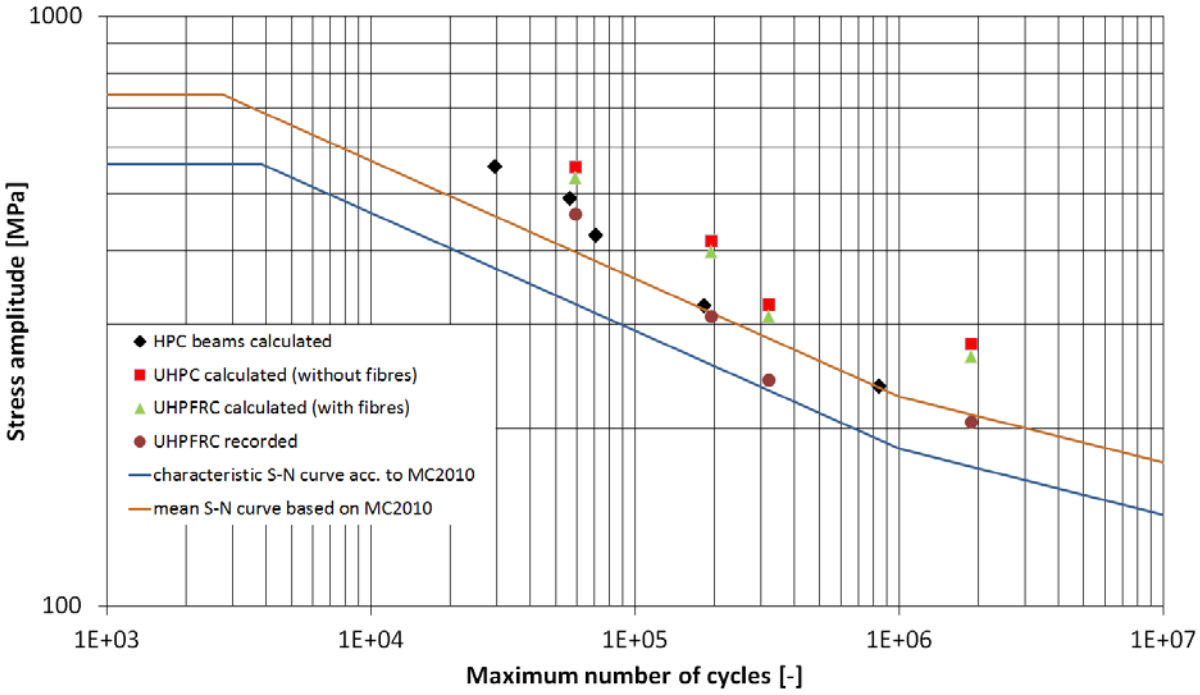

Fig. 6: S-N curves and the measured values

5. Conclusions

Two series of HSC and UHPFRC beams reinforced with high grade steel bars were tested under high-cycle fatigue loading. The pulsating load was kept constant between the minimum force of 5 to 7.5% of the monotonic load bearing capacity and an upper level of 35% to 70% of the ultimate load. All tests resulted in fatigue failure of the longitudinal reinforcement at maximum cycle numbers between 3×10^4 and 2×10^6.

A simplified approach for back-calculating the contribution of the fibres is presented. Under monotonic loading the fibre effect was about 9 to 13% with respect to the tensile stress of the longitudinal reinforcing bars. Under high-cycle fatigue loading, this effect decreased, but still plays an important role and results in an improved fatigue resistance of the beams. As seen in one test, a strongly fluctuating fibre distribution can cause torsional effects in the loaded beam structure.

The two types of tested concrete beams, rectangular HSC beams and slender UHPFRC beams with I-shaped cross-sections, both provided with high grade steel reinforcing bars, exhibited a satisfying structural response under cyclic loading. The fatigue behaviour was clearly on the safe side when applying fatigue design according to fib Model Code 2010.

Acknowledgements

The test series were performed in the frame of a research project named HiPerComp (High Performance Composites). The authors wish to acknowledge the Austrian Research Foundation (FFG) which funded the research described in this paper.

References

[1] ZHANG, Jun, STANG, Henrik. *Fatigue performance in flexure of fibre reinforced concrete.* ACI Materials Journal 95(1), 58–67, 1998. ISSN 0889-325X.

[2] LEE, M. K., BARR B. I. G. *An overview of the fatigue behaviour of plain and fibre reinforced concrete.* Cement & Concrete Composites 26(4), 299–305, 2004. ISSN 0958-9465.

[3] SALEH, F. Mofreh, YEOW, T., MACRAE, G., SCOTT A. *Effect of Steel Fibre Content on the Fatigue Behaviour of Steel Fibre Reinforced Concrete.* 7th RILEM International Conference on Cracking in Pavements, RILEM Bookseries 4, 815–825, 2012. ISSN: 2211-0844

[4] MAKITA, Tohru, BRÜHWILER, Eugen. *Tensile fatigue behaviour of Ultra-High Performance Fibre Reinforced Concrete combined with steel rebars (R-UHPFRC).* International Journal of Fatigue 59, 145–152, 2014. ISSN: 0142-1123

[5] EN 1992-1-1:2004-12 *Eurocode 2: Design of concrete structures – Part 1-1: General rules and rules for buildings, 2004.*

[6] LEUTBECHER, Torsten; FEHLING, Ekkehard. *Tensile Behavior of Ultra-High-Performance Concrete Reinforced with Reinforcing Bars and Fibers: Minimizing Fiber Content.* ACI Structural Journal 109(2), 253–264, 2012. ISSN: 0889-3241

[7] RANDL, Norbert, MÉSZÖLY, Tamás. *The effect of fibers in UHPFRC beams with longitudinal steel reinforcement.* ACI-fib Workshop Proceedings, FRC 2014 – Joint ACI-fib International Workshop, Fibre Reinforced Concrete: from Design to Structural Applications, Montréal, 2014.

[8] International Federation for Structural Concrete (fib), *Model Code for Concrete Structures 2010*. Ernst & Sohn, Lausanne, 2013. ISBN: 978-3-4330-3061-5